Confining potential in momentum space

JOHN W. NORBURY
Department of Physics, Rider College, Lawrenceville, NJ 08648, U.S.A.
DAVID E. KAHANA
Continuous Electron Beam Accelerator Facility, Newport News, VA 23606, U.S.A.
AND
KHIN MAUNG MAUNG
Department of Physics, Hampton University, Hampton, VA 23668, U.S.A. and NASA Langley Research Center, Hampton, VA 23665, U.S.A.

Received September 4, 1991

A method is presented for the solution in momentum space of the bound-state problem with a linear potential in r space. The potential is unbounded at large r leading to a singularity at small q. The singularity is integrable, when regulated by exponentially screening the r-space potential, and is removed by a subtraction technique. The limit of zero screening is taken analytically, and the numerical solution of the subtracted integral equation gives eigenvalues and wave functions in good agreement with position space calculations.

On présente une méthode pour la résolution dans l'espace des impulsions du problème des états liés, avec un potentiel linéaire dans l'espace r. Ce potentiel n'étant pas borné pour les grandes valeurs de r, on a une singularité pour les faibles valeurs de q. Ce potentiel est intégrable et peut être enlevé par une technique de soustraction, si on ajoute un écran exponentiel au potentiel dans l'espace r. La limite d'écran zéro est prise analytiquement, et la solution numérique de l'équation intégrale soustraite donne des valeurs propres et des fonctions d'onde qui sont en bon accord avec les calculs effectués dans l'espace des positions. La méthode peut facilement être généralisée pour des potentiels variant selon une loi de puissance arbitraire.
[Traduit par la rédaction]

Can. J. Phys. 70, 86 (1992)

Lattice gauge calculations (1) for static (heavy) quarks support the notion that the interquark potential in quantum chromodynamics (QCD) behaves as $V(r) \sim \lambda r$ for large r. Indeed, the linear potential has long been used in phenomenological nonrelativistic quark models of baryons and mesons (2, 3). Meson spectroscopy in particular is successfully described by a linear potential at large r, modified by spin- and colour-dependent Coulomb forces at small r. Most calculations with the linear potential are carried out in coordinate space. This is the simplest procedure for heavy-quark systems, which can perhaps be considered as nonrelativistic; however for light-quark systems it would be desirable to have a relativistic treatment. Bound-state equations in relativistic systems (4) are generally much easier to solve in momentum space, and thus we are led to consider, as a starting point for the relativistic case, the Schrödinger equation for two scalar particles interacting by a linear potential. The methods developed will generalize relatively straightforwardly to relativistic treatments.

To summarize: here, we treat the Schrödinger equation for a linear r-space potential. The method is for the most part straightforward, the only difficulty arising from the singularity of the kernel at the origin of momentum space. Previous treatments (5) have usually been approximate in the sense that the singularity was handled by screening the r-space pontential:

$$[1] \quad V(r) \sim \lambda r\, e^{-\eta r}$$

What has perhaps not been generally appreciated is that the limit $\eta \to 0$ can be taken analytically. Previous treatments keep the parameter η finite, leading to some uncertainty as to the nature of the calculated eigenvalues and wave functions. In this connection, recall that the screened linear potential does not, strictly speaking, possess true bound states, instead it has scattering resonances, which for low energy approximate the bound states of the unscreened potential. We will extract the limit of zero screening analytically, using a subtraction technique. The resulting subtracted integral equation is relatively easy to handle numerically. An alternative procedure, not employing any subtraction, and leading to a different integrodifferential equation is presented in ref. 6. Our approach is easy to implement and generalizes without difficulty to higher partial waves. The Schrödinger equation for the lth partial wave is (with the inhomogeneous term already omitted, as it will not contribute to the bound states in the limit of zero screening)

$$[2] \quad \frac{p^2}{2\mu}\phi_l(p) + \int V_l(p,p')\,\phi_l(p')\,p'^2\,dp' = E\phi_l(p)$$

Here $\mu = m_1 m_2/(m_1 + m_2)$ is the reduced mass and V_l, given by

$$[3] \quad V_l(p,p') = \frac{\lambda}{\pi}\left[\frac{Q_l'(y)}{(pp')^2} + \eta^2\frac{Q_l''(y)}{(pp')^3}\right]$$

is the lth partial-wave component of the Fourier transform of [1]:

$$[4] \quad \hat{V}(p,p') = -\frac{\lambda}{2\pi^2}\left[\frac{2}{[(p'-p)^2+\eta^2]^2} - \frac{8\eta^2}{[(p'-p)^2+\eta^2]^3}\right]$$

The variable y is given by:

$$[5] \quad y = \frac{p^2 + p'^2 + \eta^2}{2pp'}$$

$Q_l'(y)$ and $Q_l''(y)$ are the first and second derivatives (with respect to y) of the Legendre function of the second kind. To illustrate the method we specialize to s-waves, where we find by contour integration

$$[6] \quad \int V_l(p,p')p'^2\,dp' = \frac{\lambda}{\pi}\int dp'\left[Q_0'(y) + \frac{\eta^2}{pp'}Q_0''(y)\right]$$

$$= \frac{\lambda}{\pi}\left[-\frac{\pi p^2}{\eta} + \frac{\pi p^2}{\eta}\right] = 0$$

Note that when $\eta = 0$, $Q_0'(y)$ and $Q_0''(y)$ have double and quadruple poles, respectively, at $p' = p$, so that their integrals do not exist separately. Nevertheless, the two terms added together produce a function with an integrable singularity. This is illustrated in Fig. 1, which shows the kernel as a function of p' for fixed p. One observes that there is a central maximum at $p' = p$ with height scaling as $1/\eta^2$, flanked by two minima at $p' \sim p \pm 2\eta$ whose heights also scale with $1/\eta^2$. The integral vanishes [6] and this allows us to rewrite the Schrödinger equation in subtracted form

$$[7] \quad \frac{p^2}{2\mu}\phi_0(p) + \frac{\lambda}{\pi}\int\left[\frac{Q_0'(y)}{(pp')^2} + \eta^2\frac{Q_0''(y)}{(pp')^3}\right]$$

$$\times [\phi_0(p') - \phi_0(p)]p'^2\,dp' = E\phi_0(p)$$

The limit $\eta \to 0$ now exists, and may be extracted by splitting the region of integration to isolate the singularity. We write

$$[8] \quad \int dp'\left[Q_0'(y) + \frac{\eta^2}{pp'}Q_0''(y)\right][\phi_0(p') - \phi_0(p)]$$

$$= \int_0^{p-4\eta} + \int_{p-4\eta}^{p+4\eta} + \int_{p+4\eta}^{\infty}$$

$$= A + B + C$$

The limits $p \pm 4\eta$ are chosen so that all three extrema of the kernel lie in the middle region B. The explicit forms of the Legendre functions are

$$Q_0'(y) = \frac{1}{1-y^2}$$

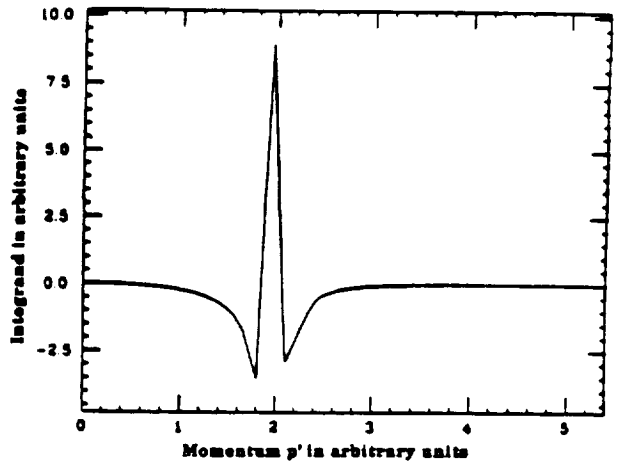

FIG. 1. The singularity structure of the kernel is shown for finite $\eta = 0.075$ with fixed $p = 2$.

$$= pp'\left[\frac{-1}{(p'-p)^2+\eta^2} + \frac{1}{(p'+p)^2+\eta^2}\right]$$

and

$$\frac{\eta^2}{pp'}Q_0''(y) = \eta^2(p^2 + p'^2 + \eta^2)$$

$$\times\left[\frac{-1}{(p'-p)^2+\eta^2} + \frac{1}{(p'+p)^2+\eta^2}\right]^2$$

It is clear that for $p' \neq p$, as is the case in the integrals A and C, the limit $\eta \to 0$ is innocuous, and may be taken immediately, indeed one has

$$[9] \quad \lim_{\eta\to 0}[A + C]$$

$$= P\int_0^{\infty} dp'\left[\frac{-4p^2p'^2}{(p'^2-p^2)^2}\right][\phi_0(p') - \phi_0(p)]$$

where P denotes as usual, the Cauchy principal value of the integral, which has been made well defined by the subtraction. The term B must be handled with care, however, since $p' = p$ inside the region of integration. Assuming $\phi(p')$ is analytic in the neighborhood of p, and making an obvious change of variable we find

$$[10] \quad \lim_{\eta\to 0} B = \lim_{\eta\to 0}\int_{-4\eta}^{4\eta} dx\left\{\left[p(p+x)\left[\frac{-1}{x^2+\eta^2} + \frac{1}{(x+2p)^2+\eta^2}\right]\left[x\phi' + \frac{x^2}{2}\phi'' + \ldots\right]\right]\right.$$

$$\left. + \left[\eta^2[(x+p)^2 + p^2 + \eta^2]\left[\frac{-1}{x^2+\eta^2} + \frac{1}{(x+2p)^2+\eta^2}\right]^2\left[x\phi' + \frac{x^2}{2}\phi'' + \ldots\right]\right]\right\} = \lim_{\eta\to 0} B1 + \lim_{\eta\to 0} B2$$

Scaling out 4η then results in

$$[11] \quad \lim_{\eta\to 0} B1 = \lim_{\eta\to 0}\int_{-1}^{1}(4\eta)\,dy\,\frac{p}{4\eta}\left(\frac{p}{4\eta} + y\right)\left(\frac{-16}{1+16y^2}\right)\left[(4\eta)y\phi' + \frac{(4\eta)^2y^2}{2}\phi'' + \ldots\right]$$

$$= [p^2\phi'(p)]\int_{-1}^{1} dy\left(\frac{-16y}{1+16y^2}\right) = 0$$

TABLE 1. Energy eigenvalues in GeV for $l = 0$, $m_1 = m_2 = 1.5$ GeV, and $\lambda = 5$ GeV^2

	N						
	8	10	12	14	16	18	Exact
E_1	5.973	5.972	5.972	5.972	5.972	5.972	5.971
E_2	10.468	10.444	10.443	10.443	10.443	10.443	10.441
E_3	14.389	14.114	14.111	14.104	14.104	14.104	14.101
E_4	18.646	17.452	17.378	17.341	17.335	17.335	17.335
E_5	23.402	21.125	20.397	20.351	20.294	20.293	20.291
E_6	27.206	25.683	23.440	23.281	23.072	23.053	23.046
E_7	33.032	31.269	27.274	26.059	25.842	25.648	25.646
E_8	44.374	36.224	32.113	29.032	28.789	27.947	28.119
E_9		40.519	38.146	33.051	31.561	30.194	30.488
E_{10}		51.774	45.309	38.067	34.428	33.340	32.769
E_{11}			49.940	44.286	38.517	36.489	34.972
E_{12}			58.588	51.893	43.615	37.309	37.109

The contribution of the second term in $B1$ clearly vanishes since it is not singular at $p' = p$, the analysis of $B2$ is similar, and we conclude that B tends to zero. Therefore the limiting form of the equation is

$$[12]\quad \frac{p^2}{2\mu}\phi_0(p) - \frac{\lambda}{\pi p^2} P \int_0^\infty dp' \left[\frac{4p^2p'^2}{(p'^2 - p^2)^2}\right][\phi_0(p') - \phi_0(p)] = E\phi_0(p)$$

We now discuss the numerical solution of [12], which is not yet a completely trivial matter, since care must be taken to obtain the Cauchy principal value. In this respect there is a difference between the linear potential and the Coulomb potential, the latter giving rise to a logarithmic singularity. For the Coulomb potential, the method used in the literature (7) is to write the Coulomb analog of [12] directly, for example, using Gaussian quadrature, as a matrix equation. Since the singularity is only logarithmic this method is successful for the Coulomb potential. Here, such an approach is not feasible. Instead, we expand ϕ_0 in a suitable set of basis functions

$$[13]\quad \phi_0(p) = \sum_n^N C_n g_n(p)$$

Inserting this expansion in [12], multiplying by $p^2 g_m(p)$ and integrating over p, we obtain

$$[14]\quad \sum_n C_n\left\{\int \frac{p^4}{2\mu} g_m(p)g_n(p)\,dp + \frac{\lambda}{\pi}\int\left[\frac{4p^2p'^2}{(p'^2 - p^2)^2}\right] g_m(p)[g_n(p') - g_n(p)]\,dp'\,dp = E\sum_n C_n \int p^2 g_m(p)g_n(p)\,dp$$

which is just the matrix equation

$$[15]\quad \sum_n A_{mn}C_n = E\sum_n G_{mn}C_n$$

The double integral over p and p' is performed by changing to variables $(p' + p)$ and $(p' - p)$. The singularity is in the integral over $(p' - p)$, so this is carried out first using Gaussian quadrature with an even number of points. This type of integration yields the Cauchy principal value automatically (8). A convenient set of functions $g(p)$ is

$$[16]\quad g_n(p) = \frac{1}{(n^2/N)^2 + p^4}$$

where N is the maximum number of functions used in expansion [13]. Figure 2 is a 3D plot of the kernel of [14], showing clearly the cancellation that leads to the principal value. Using the above method, we have calculated both eigenvalues and eigenvectors. In Table 1 the first 12 eigenvalues are listed. We used $m_1 = m_2 = 1.5$ GeV and the string tension $\lambda = 5$ GeV^2. One can see that the lower eigenvalues converge nicely as the number of functions is increased. We compare these with the eigenvalues obtained from a coordinate space calculation (integrating the equation out from $r = 0$ and in from large r, and matching the logarithmic derivatives at the classical turning point), in Table 1. The calculated eigenfunctions also agree with the coordinate-space calculation.

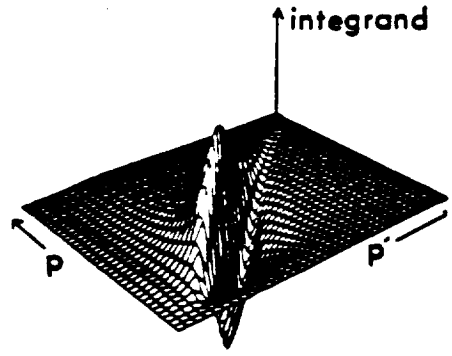

FIG. 2. A three-dimensional figure of the subtracted, regulated integrand; $\eta = 0.075$. The cancellation that produces the Cauchy principle value is evident.

In conclusion, we have treated the problem of two nonrelativistic, scalar particles interacting via a linear potential in momentum space. The relevant Schrödinger equation has a singular kernel. We have shown how after regulating the singularity by exponentially screening the r-space potential, the severity of the singularity can be reduced by a suitable subtraction, and the limit of zero screening extracted analytically. To the best of our knowledge, this point has not been generally understood in the literature. The limiting form of the equation has been treated numerically, and the results are in good agreement with more straightforward coordinate space calculations. Relativistic equations involving linear potentials involve similar singularities, so that the methods developed here will be applicable. We intend to study the relativistic quark–antiquark problem in the future. The method presented here can be generalized to higher partial waves without undue difficulty.

Acknowledgements

We are extremely grateful to Franz Gross for his generous contribution of essential ideas during all stages of this work. We would also like to thank Warren Buck and J.W.N. would like to thank Frank Cucinotta and Barry Ganapol for useful conversations. K.M.M. and J.W.N. would like to thank the Continuous Electron Beam Accelerator Facility for its hospitality. This work was supported in part by the Department of Energy through Continuous Electron Beam Accelerator Facility (D.E.K.), and by NASA grants NAG-1-1134 (J.W.N.) and NAG-1-477 (K.M.M.).

1. J. D. Stack. Phys. Rev. D: Part. Fields, **27**, 412 (1983); A. Hasenfratz and P. Hasenfratz. Ann. Rev. Nucl. Part. Sci. **35**, 559 (1985).
2. E. Eichten, K. Gottfried, T. Kinoshita, K. D. Lane, and T. M. Yan. Phys. Rev. D: Part. Fields, **17**, 3090 (1978); **21**, 203 (1980).
3. S. Godfrey and N. Isgur. Phys. Rev. D: Part. Fields, **32**, 189 (1985)
4. W. W. Buck and F. Gross. Phys. Rev. C: Nucl. Phys. **20**, 2361 (1979); F. Gross. Phys Rev. **186**, 1448 (1969); H. Crater and P. Van Alstine. Phys. Rev. D: Part. Fields **37**, 1982 (1988).
5. A. B. Henriques, B. H. Kellett, and R. G. Moorhouse. Phys. Lett. **64B**, 85 (1976).
6. J. R. Spence and J. P. Vary. Phys. Rev. D: Part. Fields **35**, 2191 (1987).
7. Y. R. Kwon and F. Tabakin. Phys. Rev. C: Nucl. Phys. **18**, 932 (1978); R. H. Landau. **27**, 2191 (1983).
8. I. H. Sloan. J. Comput. Phys. **3**, 332 (1968).

RAPID COMMUNICATION

PHYSICAL REVIEW C VOLUME 43, NUMBER 5 MAY 1991

Calculations of hadronic dissociation of ^{28}Si projectiles at 14.6A GeV by nucleon emission

Lawrence W. Townsend
National Aeronautics and Space Administration Langley Research Center, Hampton, Virginia 23665-5225

John W. Norbury
Department of Physics, Rider College, Lawrenceville, New Jersey 08648
and National Aeronautics and Space Administration Langley Research Center, Hampton, Virginia 23665-5225

Ferdous Khan
Department of Physics, Old Dominion University, Norfolk, Virginia 23529
(Received 15 November 1990)

An optical potential abrasion-ablation collision model is used to calculate hadronic dissociation cross sections for one, two, and three nucleon removal for the first time for a 14.6A GeV ^{28}Si beam fragmenting in aluminum, tin, and lead targets. These estimates are compared with recent semi-inclusive measurements. Significant differences between some calculated and measured semi-inclusive cross sections exist which cannot be resolved without measurements of the exclusive channel hadronic cross sections. Calculations for each exclusive reaction channel contributing to the semi-inclusive cross sections are presented and discussed.

Recently, the E814 Collaboration at Brookhaven National Laboratory (BNL) made a very detailed experimental study of the breakup of silicon beams at relativistic energies ($E_{\rm lab}$=14.6A GeV or $T_{\rm lab}$=13.7A GeV) using the Alternating-Gradient Synchrotron.[1] They reported cross-section measurements of one, two, and three nucleon removal by aluminum, tin, and lead targets from both electromagnetic and hadronic dissociation processes. For the electromagnetic dissociation (EMD) process, measurements of individual exclusive channel contributions were reported. Comparisons of measurements for 1p and 1n removal with calculated values obtained using the Weizsacker-Williams method of virtual quanta[2] were made, and good agreement was obtained. More recently, Llope and Braun-Munzinger[3] extended the EMD analysis to include multiple excitations of the giant dipole resonance coupled with fragmentation probabilities obtained from the standard statistical model of nuclear decay. They then use this extended calculational framework to predict exclusive EMD cross sections for many of the channels measured by the E814 Collaboration.

For the measured hadronic dissociation channels, however, no detailed analyses have been reported. In Ref. 1, simple comparisons between semi-inclusive measurements and a recent parametrization[4] of 1p and 1n geometrical calculation of single nucleon removal[5] were made. In this work, we analyze the hadronic dissociation of silicon projectile nuclei by aluminum, tin, and lead targets using an optical potential abrasion-ablation collision model which includes contributions from frictional-spectator interactions.[6] This model is used to calculate exclusive cross sections. Although no exclusive experimental hadronic cross sections were reported in Ref. 1 (the only exclusive cross sections reported were due to EMD), these calculated results are presented to stimulate interest in their experimental measurement and to facilitate further discussion in the semi-inclusive cross-section analysis.

The abrasion portion of this formalism was recently used to successfully describe single nucleon emission in relativistic nucleus-nucleus collisions.[7] Predictions of hadronic cross sections for the exclusive reaction channels measured in Ref. 1 are presented. Semi-inclusive cross sections, obtained by summing the appropriate exclusive channels, are presented and compared with the measured values reported in Ref. 1. Reasonably good agreement is obtained for the xp (x=1, 2, 3) channels. However, for the yn (y=1, 2) channels, the agreement is not as good, with the calculations generally overestimating the experimental data. Comments concerning the difficulties in resolving these differences are made, and the need for exclusive measurements of these hadronic cross sections is pointed out.

In the optical potential formalism,[6] the abrasion cross section for removal of m nucleons is

$$\sigma_{\rm abr}(A_{\rm PF}) = \binom{A_p}{m} \int d^2b [1-P(b)]^m [P(b)]^{A_{\rm PF}} , \quad (1)$$

where

$$P(b) = \exp[-A_T \sigma(e) I(b)] , \quad (2)$$

with

$$I(b) = [2\pi B(e)]^{-3/2} \int dz_0 \int d^3\xi_T \rho_T(\xi_T) \int d^3y \rho_p(b+z_0+y+\xi_T) \exp[-y^2/2B(e)] . \quad (3)$$

In Eqs. (2) and (3), b is the impact parameter, e is the two-nucleon kinetic energy in their center-of-mass frame, z_0 is the target center-of-mass position in the projectile rest frame, ξ_T denotes the target-nucleus internal coordinates, and y is the projectile-nucleon–target-nucleon relative coordinate. Methods for obtaining the appropriate nuclear distributions ρ_i $(i=P, T)$ and constituent-averaged nucleon-nucleon cross sections $\sigma(e)$ are given in Ref. 8. Values for the diffractive nucleon-nucleon scattering slope parameter $B(e)$ are obtained from the parametrization in Ref. 9. The Pauli correlation correction derived in Ref. 8 is neglected here because it is negligible for the peripheral collisions[6] being considered in this work.

Since the abraded nucleons consist of protons and neutrons, a prescription for calculating the prefragment charge dispersion is needed. The three available choices are completely correlated,[10] hypergeometric (completely uncorrelated),[11] and a model based upon the zero-point vibrations of the giant dipole resonance.[12] For the present work, we have chosen to implement the hypergeometric model, which assumes that there is no correlation at all between the neutron and proton distributions. For few nucleon removal processes, such as are being investigated here, the calculated results are not particularly sensitive to any of these particular charge dispersion methods.[13] For example, all three methods yield identical charge dispersion results for single nucleon abrasions from self-conjugate nuclei. If z out of the original Z projectile nucleus protons are abraded along with n out of the original N projectile neutrons, then the abrasion cross section becomes

$$\sigma_{\rm abr}(Z_{\rm PF},A_{\rm PF})=\frac{\binom{N}{n}\binom{Z}{z}}{\binom{A_p}{m}}\sigma_{\rm abr}(A_{\rm PF})\,, \tag{4}$$

where

$$m=n+z\,, \tag{5}$$

$$Z_{\rm PF}=Z-z\,, \tag{6}$$

$$A_{\rm PF}=A_p-m\,, \tag{7}$$

and $\binom{A_p}{m}$ denotes the usual binomial coefficient expression from probability theory. To complete the abrasion portion of the calculation, prefragment excitation energies $E_{\rm exc}$ must be estimated. We use

$$E_{\rm exc}=E_s+E_{\rm FSI}\,, \tag{8}$$

where the surface energy term (E_s) is calculated using the usual clean-cut abrasion formalism.[14] The frictional-spectator interaction (FSI) contribution $(E_{\rm FSI})$ is estimated using the methods of Ref. 11. To compute the probability that p FSI's have occurred for each abrasion of m nucleons, we use an extension of the Benesh, Cook, and Vary (BCV) prescription for estimating escape probabilities of abraded nucleons rather than the usual assumed value of one-half.[6,11] Therefore, the abrasion cross section for a prefragment of isotopic species $(Z_{\rm PF},A_{\rm PF})$ which has undergone p FSI's is given by

$$\sigma_{\rm abr}(Z_{\rm PF},A_{\rm PF},p)=\binom{m}{p}(1-P_{\rm esc})^p(P_{\rm esc})^{m-p}\times\sigma_{\rm abr}(Z_{\rm PF},A_{\rm PF})\,, \tag{9}$$

where $P_{\rm esc}$ is the BCV probability that an abraded nucleon escapes without undergoing any frictional-spectator interactions.[5] For the reactions considered herein, $P_{\rm esc}\approx 0.7$.

Depending upon the excitation energy, the excited prefragment will decay by emitting one or more nucleons, composites, or gamma rays. The probability $a_{ij}(p)$ for formation of a specific final fragment of type i as a result of the deexcitation of a prefragment of type j which has undergone p frictional-spectator interactions is obtained using the EVA-3 computer code.[12] For $m=1$ or 2 and $p=0$ (no FSI), the values of $E_{\rm exc}$ are less than 3 MeV for all targets and no particle emission occurs. Hence, the calculated cross sections for ^{27}Si$+n$, ^{26}Si$+2n$, ^{27}Al$+p$, and ^{26}Mg$+2p$ arise solely from the abrasion process. Whenever one or more FSI's ($p=1$, 2) occur for a fragmenting silicon nucleus, an additional (average) excitation energy of 31 MeV per FSI (computed using the methods of Ref. 11) is deposited in the prefragment. When these resultant excitation energies are used as inputs into the EVA-3 code, the cross sections for the ^{25}Mg$+2p+n$ and the ^{25}Al$+p+2n$ final states are so large that all calculated xn or xp ($x=1$, 2) semi-inclusive cross sections significantly overestimate the present experimental measurements. In earlier work[15] on a semiempirical fragmentation code which used this same FSI model, it was noted that improved agreement between calculations and all available experimental data were obtained if values of excitation energy were increased above those obtained from the methods of Ref. 11. In this work, we observed that treating $E_{\rm FSI}$ as a free parameter and increasing its value by 15 MeV reduced the cross sections for the ^{25}Mg$+2p+n$ and ^{25}Al$+p+2n$ channels—thereby improving the semi-inclusive cross-section predictions. Therefore, the final hadronic cross section for production of the type i isotope is given by

$$\sigma_{\rm nuc}(Z_i,A_i)=\sum_j\sum_{p=0}^{m}a_{ij}(p)\sigma_{\rm abr}(Z_j,A_j,p)\,, \tag{10}$$

where the summation over j accounts for the contributions to i from different prefragment species j, and the summation over p accounts for the effects of the different excitation energies resulting from FSI's.

Estimated exclusive cross sections obtained using the fragmentation model described herein are separately listed in Table I for each target. To compare our predictions with the semi-inclusive hadronic cross-section measurements (Fig. 4 of Ref. 1), we sum the exclusive channels listed in Table I for each of the relevant nucleon emission reactions. For example, the $1p$ semi-inclusive calculation is the sum of the exclusive channel cross sections for the ^{27}Al$+p$, ^{26}Al$+p+n$, ^{25}Al$+p+2n$, and the ^{24}Al$+p+3n$ reactions. Similarly, the $1n$ semi-inclusive calculation is the sum of the ^{27}Si$+n$, ^{26}Al$+p+n$, ^{25}Mg$+2p+n$, and ^{24}Na$+3p+n$ exclusive channels. The calculated results for xn ($x=1$, 2) and yp ($y=1$, 2, 3) semi-inclusive cross sections are plotted in Fig. 1 along with the BNL experimental measurements from Fig. 4 of Ref. 1. Except for the $1p$ datum for the lead target, all calculated proton cross sections are in reasonably good agreement with the experimental data. Comparing the calculated and experi-

TABLE I. Exclusive channel hadronic dissociation cross-section calculations.

	Cross section (mb) with target nucleus		
Channel	Aluminum	Tin	Lead
^{27}Si+n	99.1	126.4	134.4
^{27}Al+p	99.1	126.4	134.4
^{26}Si+2n	17.9	22.3	23.9
^{26}Al+p+n	38.9	48.2	51.7
^{26}Mg+2p	17.9	22.3	23.9
^{25}Al+p+2n	1.5	2.1	2.3
^{25}Mg+2p+n	13.8	20.1	21.8
^{25}Na+3p	0.3	0.4	0.4
^{24}Al+p+3n	0.1	0.2	0.2
^{24}Mg+2p+2n	30.7	44.2	47.5
^{24}Na+3p+n	10.2	14.5	15.6

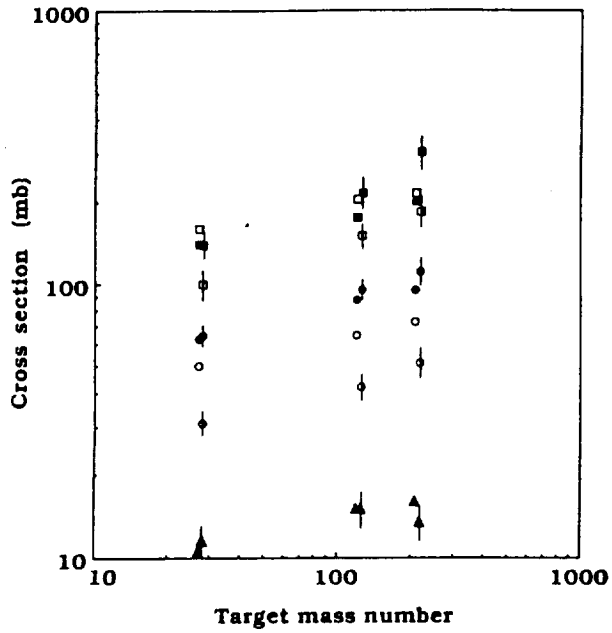

FIG. 1. Hadronic dissociation cross sections vs target mass number. The experimental data point symbols include error bars; the theoretical calculation point symbols do not. 1p is represented by a solid square, 1n by an open square, 2p by a solid circle, 2n by an open circle, and 3p by a solid triangle.

mental neutron removal cross sections, however, we note that the agreement is not as good. There the calculations systematically overestimate the measurements by nearly 50%. Since the experimental data were not corrected for detector acceptance limitations,[16] the observed trend for calculated cross sections to generally be larger than measured ones is expected because the experimental data are likely to underestimate the actual cross sections by an as yet unknown amount. Resolution of these discrepancies is therefore hampered by the lack of exclusive channel measurements and detector acceptance corrections, which would enable the source(s) of any differences to be pinpointed.

For the 1n removal calculations, the main contribution (nearly half) to these cross sections for each target arises from the ^{27}Si+n exclusive channel when no FSI occur. Simple modifications to the current calculation model, such as using the Rasmussen[11] FSI escape probability ($P_{esc} \equiv 0.5$), would reduce the neutron cross-section differences; however, the calculated proton removal cross sections would also be reduced, destroying the agreement that presently exists between theory and experiment. A potential source for part of the difference between neutron and proton removal cross sections, not accounted for by the theory, is the difference in removal threshold energies. A proton, being less tightly bound, should have a larger removal cross section than a neutron. To test this hypothesis, we turn to the earlier fragmentation measurement of carbon and oxygen beams by Lindstrom *et al.*[17] which provide a fairly complete data set. Correcting their measurements for EMD contributions using Ref. 18, we find that the exclusive 1p removal channel (^{15}N or ^{11}B formation) is only 10%–20% larger than the exclusive 1n removal channel (^{15}O or ^{11}C). Adding the other 1n and 1p exclusive channels (^{14}N, ^{13}N, ^{13}C, ^{10}C, etc.) to estimate experimental 1n and 1p inclusive cross sections yields much smaller differences between them—unlike the recent ^{28}Si measurements[1] where the 1p semi-inclusive cross sections are substantially larger than the 1n cross sections. From a binding energy point of view, this may result from the fact that the ^{11}C-^{11}B binding-energy difference is smaller than that for ^{27}Si-^{27}Al. A way to incorporate proton-neutron binding-energy differences into the present model may be to use different nuclear distributions for the proton and neutron densities. Such efforts are considered in Refs. 19 and 20. Recent work[21,22] has shown how the binding energy is directly influenced by the nuclear density. In principle, then, one could model the proton-neutron densities of ^{28}Si to fit the observed binding-energy differences. However, this particular method is beyond the scope of the present treatment. Instead, possible changes to the calculated cross sections, resulting from neutron-proton density differences, were modeled by reducing the half-density radius of the ^{28}Si neutron distribution by 0.5 fm. The calculated neutron cross sections were reduced, as anticipated, but by only a few millibarns (less than 10 mb for all targets). These reductions were not large enough to account for the reported differences between measured semi-inclusive proton and neutron removal channels. Clearly, exclusive channel experimental measurements for ^{28}Si hadronic cross sections, which are presently being analyzed,[16] would substantially aid efforts to resolve the differences between calculation and experimental measurements.

The authors wish to thank Dr. H. Takai and Dr. P. Braun-Munzinger for useful discussions. This work was partly supported by NASA Grants No. NCCI-42 and No. NAG-1-1134.

[1]E814 Collaboration, J. Barrette *et al.*, Phys. Rev. C **41**, 1512 (1990).

[2]J. D. Jackson, *Classical Electrodynamics* (Wiley, New York, 1975).

[3]W. J. Llope and P. Braun-Munzinger, Phys. Rev. C **41**, 2644 (1990).

[4]C. Brechtmann, W. Heinrich, and E. V. Benton, Phys. Rev. C **39**, 2222 (1989).

[5]C. J. Benesh, B. C. Cook, and J. P. Vary, Phys. Rev. C **40**, 1198 (1989).

[6]L. W. Townsend, J. W. Wilson, F. A. Cucinotta, and J. W. Norbury, Phys. Rev. C **34**, 1491 (1986).

[7]John W. Norbury and Lawrence W. Townsend, Phys. Rev. C **42**, 1775 (1990).

[8]L. W. Townsend, Can. J. Phys. **61**, 93 (1983); L. W. Townsend, J. W. Wilson, and J. W. Norbury, *ibid.* **63**, 135 (1985).

[9]F. E. Ringia, T. Dobrowolski, H. R. Gustafson, L. W. Jones, M. J. Longo, E. F. Parker, and Bruck Cork, Phys. Rev. Lett. **28**, 185 (1972).

[10]J. D. Bowman, W. J. Swiatecki, and C. F. Tsang, Lawrence Berkeley Laboratory Report No. LBL-2908, 1973 (unpublished).

[11]Luiz F. Oliveira, Raul Donangelo, and John O. Rasmussen, Phys. Rev. C **19**, 826 (1979).

[12]D. J. Morrissey, L. F. Oliveira, J. O. Rasmussen, G. T Seaborg, Y. Yariv, and Z. Fraenkel, Phys. Rev. Lett. **43**, 113 (1979).

[13]Lawrence W. Townsend and John W. Norbury, National Aeronautics and Space Administration Technical Memorandum No. TM-86340, 1985 (unpublished).

[14]J. Gosset, H. H. Gutbrod, W. G. Meyer, A. M. Poskanzer, A. Sandoval, R. Stock, and G. D. Westfall, Phys. Rev. C **16**, 629 (1977).

[15]John W. Wilson, Lawrence W. Townsend, and Forooz F. Badavi, Nucl. Instrum. Methods Phys. Res. Sect. B **18**, 225 (1987).

[16]H. Takai (private communication).

[17]P. J. Lindstrom, D. E. Greiner, H. H. Heckman, Bruce Cork, and F. S. Bieser, Lawrence Berkeley Laboratory Report No. LBL-3650, 1975 (unpublished).

[18]J. W. Norbury, Phys. Rev. C **40**, 2621 (1989).

[19]G. Bertsch, H. Esbensen, and A. Sustich, Phys. Rev. C **42**, 758 (1990).

[20]G. Bertsch, B. A. Brown, and H. Sagawa, Phys. Rev. C **39**, 1154 (1989).

[21]J. W. Negele, Phys. Rev. C **1**, 1260 (1970), see Fig. 5.

[22]X. Campi and D. W. Sprung, Nucl. Phys. A **194**, 401 (1972), see Fig. 12.